La Mar, G. N., de Ropp, J. S., Smith, K. M., & Langry, K. C. (1981) *J. Biol. Chem. 256*, 237–243.
La Mar, G. N., de Ropp, J. S., Latos-Grazynskk, L., Balch, A. L., Johnson, R. B., Smith, K. M., Parish, D. W., & Cheng, R.-J. (1983) *J. Am. Chem. Soc. 105*, 785–787.
Lauffer, R. B., Antanaitis, B. C., Aisen, P., & Que, L., Jr. (1983) *J. Biol. Chem. 258*, 14212–14218.
Lecomte, J. T. J., & La Mar, G. N. (1986) *Eur. Biophys. J. 13*, 373–381.
Morrison, M., & Schonbaum, G. R. (1976) *Annu. Rev. Biochem. 45*, 861–888.
Nicholls, P. (1962) *Biochim. Biophys. Acta 60*, 217–226.
Noggle, J. H., & Shirmer, R. E. (1971) *The Nuclear Overhauser Effect*, Academic, New York.
Pande, U., La Mar, G. N., Lecomte, J. T. J., Ascoli, F., Brunori, M., Smith, K. M., Pandey, R. K., Parish, D. W., & Thanabal, V. (1986) *Biochemistry 25*, 5638–5646.
Poulos, T. L., & Kraut, J. (1980) *J. Biol. Chem. 255*, 8199–8205.
Redfield, A. G., Kunz, S. D., & Ralph, E. E. (1975) *J. Magn. Reson. 19*, 114–117.
Sakurada, J., Takahashi, S., & Hosoya, T. (1986) *J. Biol. Chem. 261*, 9657–9662.
Satterlee, J. D. (1986) *Annu. Rep. NMR Spectrosc. 17*, 79–178.
Satterlee, J. D., & Erman, J. E. (1981) *J. Biol. Chem. 256*, 1091–1093.
Slichter, C. P. (1978) *Principles of Magnetic Resonance*, Chapter 2, Springer-Verlag, Berlin.
Thanabal, V., de Ropp, J. S., & La Mar, G. N. (1986) *J. Am. Chem. Soc. 108*, 4244–4245.
Thanabal, V., de Ropp, J. S., & La Mar, G. N. (1987a) *J. Am. Chem. Soc. 109*, 265–272.
Thanabal, V., de Ropp, J. S., & La Mar, G. N. (1987b) *J. Am. Chem. Soc. 109*, 7516–7525.
Thanabal, V., de Ropp, J. S., & La Mar, G. N. (1988) *J. Am. Chem. Soc.* (in press).
Unger, S. W., Lecomte, J. T. J., & La Mar, G. N. (1985) *J. Magn. Reson. 64*, 521–526.
Welinder, K. G. (1985) *Eur. J. Biochem. 151*, 497–504.
Yonetani, T., & Ray, G. S. (1965) *J. Biol. Chem. 240*, 4503–4508.

Two-Dimensional NMR Studies of the Porcine Muscle Adenylate Kinase†

Werner Klaus,‡ Michael Scharf, Sabine Zimmermann, and Paul Rösch*
Max-Planck-Institute for Medical Research, Department of Biophysics, Jahnstrasse 29, D-6900 Heidelberg 1, FRG
Received October 27, 1987; Revised Manuscript Received March 11, 1988

ABSTRACT: Porcine adenylate kinase was subjected to one- and two-dimensional proton NMR studies in order to identify amino acid spin systems and obtain sequence-specific resonance assignments. With a combination of results from a map of side-chain distances resulting from the refined X-ray crystallographic data and nuclear Overhauser effect spectroscopy (NOESY), assignments are suggested for all the aromatic spin systems.

Adenylate kinase (ATP:AMP phosphotransferase, AK;[1] EC 2.7.4.3) catalyzes the transfer of the terminal phosphoryl group from adenosine triphosphate to adenosine monophosphate in the presence of a divalent metal ion, physiologically Mg^{2+}, according to (Noda, 1973)

$$ATP{\cdot}Mg^{2+} + AMP \leftrightarrow ADP{\cdot}Mg^{2+} + ADP$$

The three-dimensional structure of the substrate-free porcine muscle protein (AK1) is well-known from X-ray studies (Schulz et al., 1974). The crystal structure of the yeast adenylate kinase (AK_y) loaded with the presumed bisubstrate analogue AP_5A was determined only recently (Egner et al., 1987).

Although there is plenty of evidence that the AP_5A complex of pig AK1 mimics the active structure of the enzyme, evidence for this property of the corresponding yeast or *Escherichia coli* adenylate kinase (AK_e) complex is less clear (Lienhard & Secemski, 1973; Feldhaus et al., 1975). NMR studies on the location of the nucleotide binding sites in mammalian AK1 were performed (Smith & Mildvan, 1982; Fry et al., 1985, 1987). The nucleotide sites as derived from these NMR studies are incompatible with the ones obtained from the X-ray studies of the $AK_y{\cdot}AP_5A{\cdot}Mg^{2+}$ complex crystal structure. Thus, the location of the two nucleotide binding sites is still under debate.

The NMR studies suffer from, among other things, the fact that only sequence-specific resonance assignments for the imidazole C2 proton of His^{189} and the C2 and C4 protons of the imidazole ring of His^{36} were obtained in porcine AK1 (McDonald et al., 1975; Kalbitzer et al., 1982). Several spin systems of aromatic side chains could be identified at 360 MHz (Rösch & Gross, 1985). In order to obtain more sequence-specific resonance assignments of the porcine AK1 proton NMR spectrum in the aromatic region, resolve some ambiguities in earlier work, and get spin system identifications in the aliphatic region we undertook two-dimensional NMR

† This work was supported by the Deutsche Forschungsgemeinschaft with Grants Ro617/1-1 and Ro617/1-2.
‡ Present address: Gesellschaft für biotechnologische Forschung, D-3300 Braunschweig, FRG.

[1] Abbreviations: AK, adenylate kinase (EC 2.7.4.3.); AP_5A, P^1,P^5-diadenosine pentaphosphate; COSY, correlated spectroscopy; DQF, double quantum filtered; DSS, 2,2-dimethyl-2-silapentane-5-sulfonate; NMR, nuclear magnetic resonance; NOESY, nuclear Overhauser effect spectroscopy; TOCSY, totally correlated spectroscopy; TQF, triple quantum filtered.

0006-2960/88/0427-5407$01.50/0

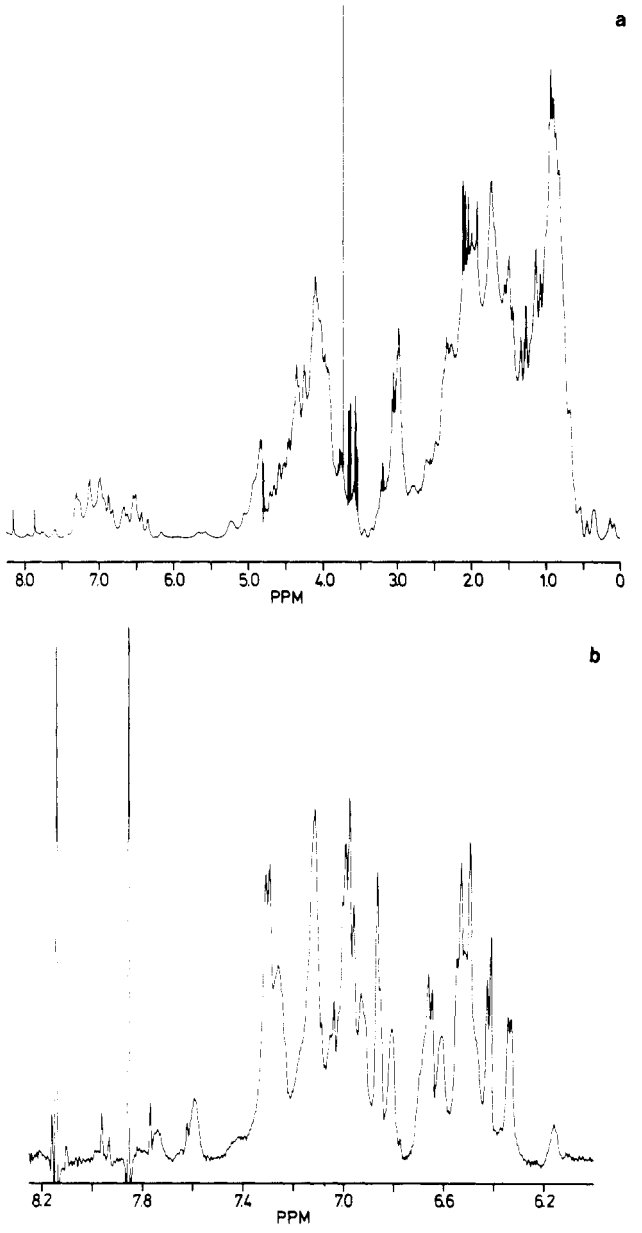

FIGURE 1: (a) ^{1}H NMR spectrum of the porcine muscle adenylate kinase: protein concentration, 1 mM; buffer, potassium phosphate, 50 mM, pH 6.2; temperature, 300 K. (b) Region of the aromatic resonances from (a). Multiplication of free induction decay with $\exp(at - bt^2)$, $a = 10.0$ and $b = 0.3$.

studies of this protein at 500 MHz.

Materials and Methods

Porcine AK1 was purified and the activity checked as reported previously (Barzy & Michelson, 1983; Tomasselli & Noda, 1980). The protein was stored in freeze-dried form at 253 K after extensive dialysis against potassium phosphate at pH 6.2 in the presence of traces of sodium azide. Final buffer concentration was approximately 50 mM in all experiments. For the NMR studies, the protein was dissolved in 99.8% D_2O, freeze-dried, and redissolved in 99.96% D_2O. The activity of the protein was not reduced after this procedure. The final protein concentration was determined by measuring the difference between the optical densities at 234.5 and 228.5 nm (Ehresman et al., 1973). For two-dimensional NMR studies we used samples with approximately 2.5 mM protein. This seemed to be the best compromise between achievable resolution, which goes down at higher protein concentrations, and necessary amount of protein to get decent signal-to-noise ratios.

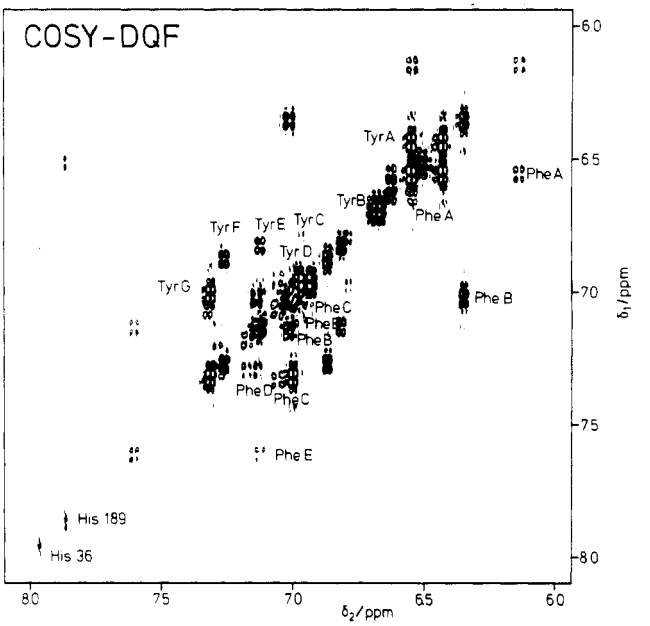

FIGURE 2: Region of the aromatic resonances from the DQF-COSY spectrum of AK1: protein concentration, 2.5 mM; other conditions as in Figure 1.

All spectra were acquired on a Bruker AM 500 spectrometer. Temperature was regulated by a stream of dry air and controlled with a Bruker VT 1000 temperature control unit. The residual HDO resonance was suppressed by continuous irradiation (except acquisition) at the HDO frequency. All spectra were referenced to internal 2,2-dimethyl-2-silapentane-5-sulfonate (DSS). A 0.4-mL aliquot of sample in a 5-mm tube and a 5-mm probe were used in all experiments. Parameters for the two-dimensional spectra were as follows: time–domain data matrix, 4K × 512 points; number of scans, typically 256; filter function applied prior to Fourier transformation, sine bell or shifted ($\pi/32$) sine bell; mixing times for totally correlated spectroscopy (TOCSY), 40 ms, for nuclear Overhauser effect spectroscopy (NOESY), 150 ms. Attempts to shorten the mixing time in the NOESY spectra gave unsatisfactory results.

We used the commercial software on an Aspect 3000 computer for spectrometer control. NMR data processing was performed on a PCS 9940 computer with a software package obtained from R. Kaptain, Utrecht, and modified and implemented in the C-programming language under the UNIX operating system by us. The distance map from the X-ray data was built with a program running in Modula-2 on an ATARI 1040 ST system connected to a mainframe DEC VAX 8600.

Results and Discussion

The resonances of the proton NMR spectrum of porcine adenylate kinase are very well resolved for a protein this size (Figure 1a). The aromatic region reveals several doublets from tyrosyl and phenylalanyl ring spin systems (Figure 1b).

Residues with Aromatic Side Chains. Inspection of the phase-sensitive, double-quantum-filtered COSY (DQF-COSY) spectrum of Phe, Tyr, and His side chains of the Porcine AK1 allows identification of all ring spin systems in the protein. These belong to five phenylalanyl residues (Phe^A to Phe^E in the figure), seven tyrosyl residues (Tyr^A to Tyr^G in the figure), and two histidyl residues. The C2H resonances of the latter were assigned earlier to His^{36} and His^{189}, respectively (McDonald et al., 1975) (Figure 2). Three out of the five phenylalanyl rings could also be detected in the totally correlated spectrum (TOCSY), which reveals correlations be-

Table I: Proton Chemical Shifts (ppm) of Amino Acids with Aromatic Side Chains (under the Conditions of Figure 2)

	ring protons			β_1	β_2	α
His^{36}	8.16 (C2H)	6.89 (C4H)		3.92	3.79	5.08
His^{189}	7.88	6.52		3.03	2.96	4.18
Phe^{A}	6.64 (C2/6H)	6.54 (C3/5H)	6.18 (C4H)			5.59
Phe^{B}	6.35	7.02	7.14	3.13	3.04	4.16
Phe^{C}	7.34	7.07	6.96			
Phe^{D}	7.29	7.18	7.14			4.44
Phe^{E}	7.60	7.13	6.98	2.99	3.11	4.85
Tyr^{A}	6.55	6.43				4.61
Tyr^{B}	6.68	6.75		3.14	3.12	4.26
Tyr^{C}	6.97	6.80				4.18
Tyr^{D}	6.98	6.94				5.69
Tyr^{E}	7.12	6.82				4.20
Tyr^{F}	7.27	6.88		2.26	2.55	4.29
Tyr^{G}	7.31	7.00		3.06	3.28	4.06

tween the A and X resonances of a three-spin AMX system (Bax & Davis, 1985) (not shown). TOCSY thus helped to unequivocally differentiate between the ortho and para proton resonances of the phenylalanyl ring systems. As in other cases, it was not possible to trace the resonances of any of the aromatic side-chain protons to the β- and α-proton resonances in the COSY spectrum. In order to detect these connectivities we had to rely on the NOESY spectrum, which allowed the determination of the chemical shifts of the α- and β-proton resonances in several cases via the dipolar interactions of these protons with the protons of the respective ring spin systems. In this way it was possible to elucidate the complete spin systems of both His residues, two out of the five Phe residues, and three out of the seven Tyr residues. The chemical shift of all but one of the α-proton resonances of the Phe, Tyr, and His residues could be determined (Table I).

Residues with Aliphatic Side Chains. Chemical shifts and connectivities of the resonances of spin systems of the aliphatic amino acids are much more difficult to determine. In the region between ~3.0 and 5.0 ppm only α-proton and β-proton resonances are to be expected (Wüthrich, 1986). Several Gly and Ser side chains could be detected in this region by comparison of the DQF-COSY spectrum in D_2O, the triple-quantum-filtered (TQF) COSY spectrum (Rance & Wright, 1986) in D_2O, and the TQF-COSY spectrum in H_2O. In the DQF-COSY spectrum, the cross-peaks due to α-proton/β-proton coupling of several amino acids as well as those due to the α-proton/α-proton coupling of the Gly residues appear in this region (Figure 3). The cross-peaks originating from the Gly α-protons can be distinguished from the cross-peaks from other amino acid proton resonances by collection of a TQF-COSY spectrum in H_2O solution, which shows the connectivities between the NH proton and the two nonequivalent α protons. This feature is unique to the Gly spin system. On the other hand, a TQF-COSY spectrum collected in D_2O shows only cross-peaks from serine α-proton/β-proton couplings in this region (Figure 4), because all other resonances expected in this part of the spectrum are either two-spin systems or three-spin systems ILS with $J_{IS} = 0.0$, preventing excitation of triple-quantum coherences. In this way, 4 Ser spin systems out of 9 in porcine AK1 and 5 out of 19 Gly spin systems could be identified (Table II). In the same region of the DQF-COSY spectrum, cross-peaks originating from the α-proton/β-proton coupling of Thr and Ala residues can be detected. In the DQF-COSY spectrum of porcine AK1, five of the β-proton resonances are connected via cross-peaks to the methyl proton resonance region, thus revealing complete threonyl spin systems (Table II).

Sequence-Specific Assignments. For a protein the size of adenylate kinase it is, unfortunately, not possible to resort to the well-known COSY and NOESY chain-tracing procedures for sequence-specific proton resonance assignments in proteins (Wüthrich, 1986). We thus had to employ a comparison of

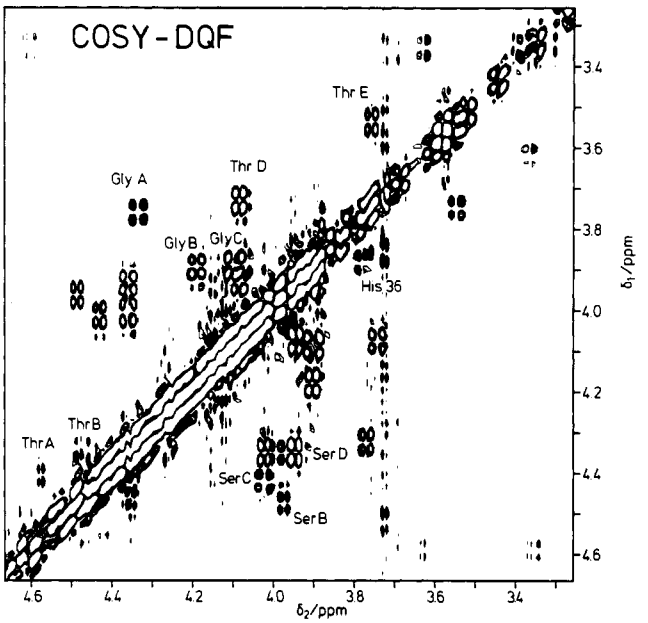

FIGURE 3: Gly region of the DQF-COSY spectrum of AK1 as in Figure 2.

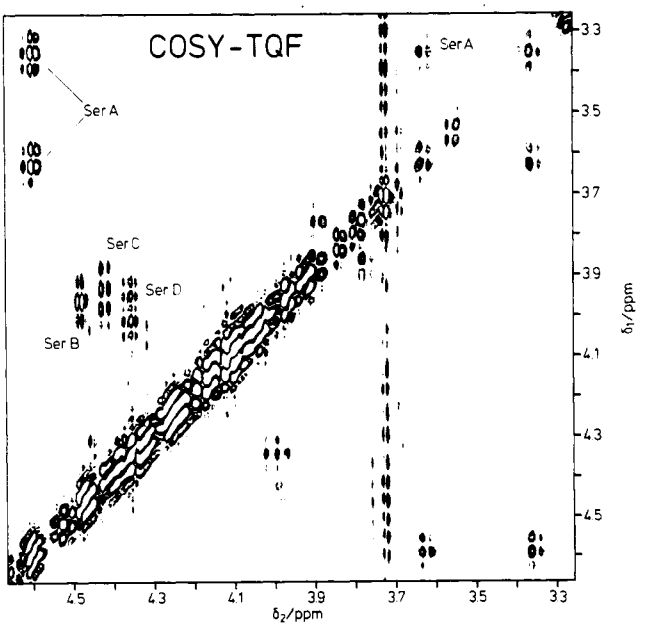

FIGURE 4: Same region as in Figure 3 of TQF-COSY spectrum: conditions as in Figure 2.

Table II: Chemical Shifts of Resonances (ppm) from Gly and Ser Residues (under the Conditions of Figure 2)

	α_1	β_1	β_2
Ser^A	4.61	3.64	3.38
Ser^B	4.48	3.96	3.96
Ser^C	4.42	3.98	3.93
Ser^D	4.36	4.01	3.96
	α_1	α_2	NH
Gly^A	4.33	3.77	
Gly^B	4.19	3.89	
Gly^C	4.10	3.88	
Gly^D	4.05	3.90	8.30
Gly^E	3.20	3.20	7.72
Gly^F	3.22	3.22	7.51
	α	β	γ
Thr^A	4.58	4.42	1.19
Thr^B	4.36	4.48	1.46
Thr^C	4.21	4.38	1.28
Thr^D	4.03	3.96	1.34
Thr^E	3.73	3.59	1.05

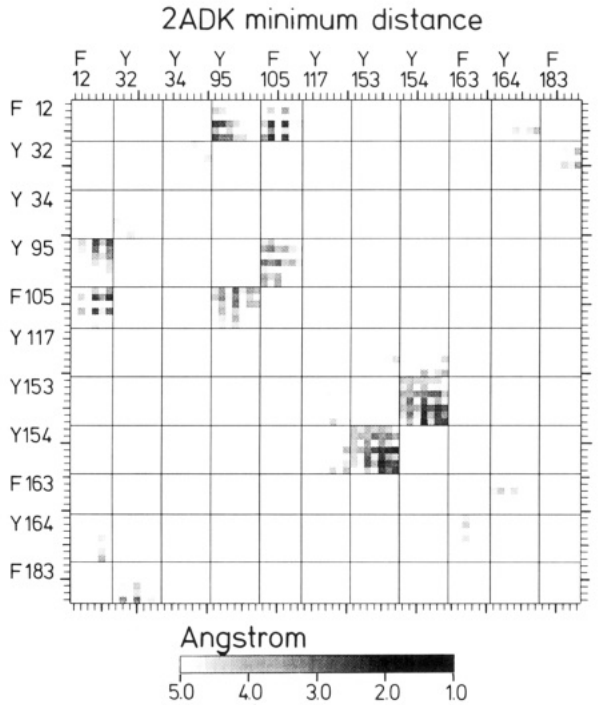

FIGURE 5: Map of proton–proton distances of the aromatic residues of porcine AK1 as derived from the X-ray structure. Horizontal and vertical axes are labeled with residue numbers. Atoms within residues are listed in the order (top to bottom and left to right): C_γ, C_δ, C_ϵ, and C_ζ (F) or OH (Y). Darker shade represents closer distance, as indicated in the gray-tone scale.

the upper limits of distances between protons of identified spin systems, information contained in the NOESY spectrum, and the structure information from the X-ray crystallographic data. As no proton–proton distance information is available from the X-ray studies, we arranged the ring part of all aromatic side chains in an X-ray structure derived carbon–carbon distance map (Figure 5). Inspection of this map shows that in a 0.5-nm radius of carbons of five aromatic side chains other aromatic side-chain carbons can be found. The value of 0.5 nm is something like the generally accepted upper distance limit between protons in proteins whose resonances show cross-peaks in the NOESY spectrum under the usual experimental conditions (Wüthrich, 1986). We thus would expect to detect several cross-peaks within the region of the aromatic side-chain resonances in the NOESY spectrum. Indeed, the NOESY spectrum of porcine AK1 (Figure 6) shows four

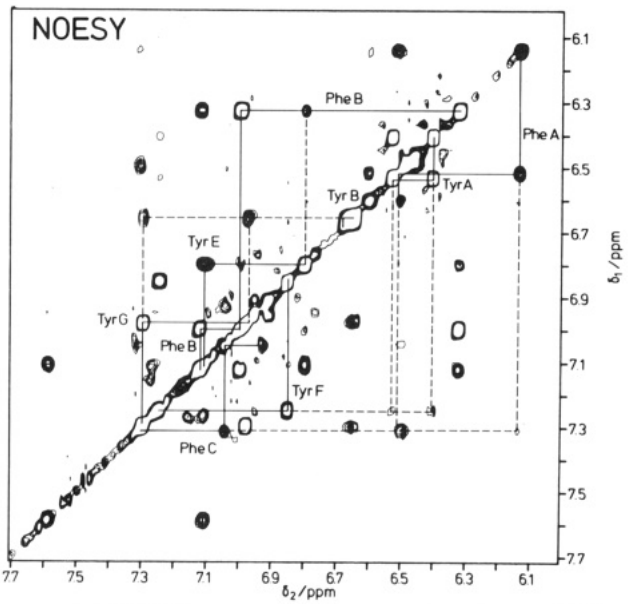

FIGURE 6: NOESY spectrum of the aromatic region: solid lines represent COSY connectivities, broken lines NOESY connectivities; conditions as in Figure 2.

Table III: Tyr and Phe Resonance Assignments As Determined by Comparison of the NOESY Cross-Peaks with the Distance Information of Figure 5

Tyr^A	Tyr^{32} or Tyr^{34}	Phe^A	Phe^{12} or Phe^{105}
Tyr^B	Tyr^{153} or Tyr^{154}	Phe^B	Phe^{163}
Tyr^C	Tyr^{95} or Tyr^{117}	Phe^C	Phe^{12} or Phe^{105}
Try^D	Tyr^{95} or Tyr^{117}	Phe^D	Phe^{90} or Phe^{183}
Tyr^E	Tyr^{164}	Phe^E	Phe^{90} or Phe^{183}
Tyr^F	Tyr^{32} or Tyr^{34}		
Tyr^G	Tyr^{153} or Tyr^{154}		

cross-peaks between proton resonances from the ring part of aromatic amino acids that can easily be correlated with side chains from aromatic residues whose mutual proximity is known to be closer than 0.5 nm from the distance map. There are two pairs of Tyr residues that show cross-peaks in the aromatic part of the NOESY spectrum, namely, Tyr^B-Tyr^G and Tyr^A-Tyr^F. These obviously correspond to the pairs Tyr^{32}-Tyr^{34} and Tyr^{153}-Tyr^{154} in the distance map. According to the crystallographic data, the distance between the protons of the aromatic rings of Tyr^{153} and Tyr^{154}, which are located at the end of an α-helix, is smaller than the distance between the aromatic rings of Tyr^{32} and Tyr^{34}, which are located in a β-sheet. We thus suggest assignment of the tyrosine pair with stronger cross-peaks to the tyrosine pair with the smaller distance according to the crystallographic data. Only two aromatic side-chain protons from phenylalanyl residues give rise to an interresidue cross-peak in the aromatic region of the NOESY spectrum, namely, Phe^A and Phe^C. Thus, these phenylalanyl residues correspond to residues Phe^{12} and Phe^{105} in the protein sequence. The cross-peak between Phe^B and Tyr^E can than be explained by assigning Tyr^E to Tyr^{164} and Phe^B to Phe^{163}. The assignments are summarized in Table III.

ACKNOWLEDGMENTS

We thank Prof. G. Schulz, Freiburg for access to the refined X-ray structural data.

Registry No. His, 71-00-1; Phe, 63-91-2; Tyr, 60-18-4; Ser, 56-45-1; Gly, 56-40-6; Thr, 72-19-5; AK, 9013-02-9.

REFERENCES

Barzy, D., & Michelson, S. (1983) *FEBS Lett. 153*, 280–284.

Bax, A., & Davis, D. G. (1985) *J. Magn. Reson. 65*, 355–360.
Berghäuser, J., & Schirmer, R. H. (1978) *Biochim. Biophys. Acta 537*, 454–463.
Egner, U., Tomasselli, A. G., & Schulz, G. E. (1987) *J. Mol. Biol. 195*, 649–658.
Ehresman, B., Imbault, P., & Weil, J. H. (1973) *Anal. Biochem. 54*, 454–463.
Feldhaus, P., Fröhlich, T., Goody, R. S., Isakov, M., & Schirmer, R. H. (1975) *Eur. J. Biochem. 57*, 197–204.
Fry, D. C., Kuby, S. A., & Mildvan, A. S. (1985) *Biochemistry 24*, 4680–4694.
Fry, D. C., Kuby, S. A., & Mildvan, A. S. (1987) *Biochemistry 26*, 1645–1655.
Kalbitzer, H. R., Marquetant, R., Rösch, P., & Schirmer, R. H. (1982).
Lienhard, G. E., & Secemski, I. I. (1973) *J. Biol. Chem. 248*, 1121–1123.
McDonald, G. G., Cohn, M., & Noda, L. (1975) *J. Biol. Chem. 250*, 6947–6954.
Noda, L. (1973) *Enzymes, 3rd ed. 8*, 279–305.
Rance, M., & Wright, P. E. (1986) *J. Magn. Reson. 66*, 372–378.
Rösch, P., & Gross, K. H. (1985) *J. Mol. Biol. 182*, 341–345.
Schulz, G. E., Elzinga, M., Marx, F., & Schirmer, R. H. (1974) *Nature (London) 250*, 120–123.
Schulz, G. E., Schiltz, E., Tomasselli, A. G., Frank, R., Brune, M., Wittinghofer, A., & Schirmer, R. H. (1986) *Eur. J. Biochem. 161*, 127–132.
Smith, G. M., & Mildvan, A. S. (1982) *Biochemistry 21*, 6119–6123.
Tomasselli, A. G., & Noda, L. H. (1980) *Eur. J. Biochem. 103*, 481–491.
Wüthrich, K. (1986) *NMR of Proteins and Nucleic Acids* Wiley, New York.

The Copper Sites of Dopamine β-Hydroxylase: An X-ray Absorption Spectroscopic Study†

Robert A. Scott,*,‡ Richard J. Sullivan,§ Walter E. DeWolf, Jr.,*,∥ Roland E. Dolle,∥,⊥ and Lawrence I. Kruse*,∥,⊥

Departments of Chemistry and Biochemistry and Center for Metalloenzyme Studies, University of Georgia, Athens, Georgia 30602, School of Chemical Sciences, University of Illinois, Urbana, Illinois 61801, and Department of Medicinal Chemistry, Research and Development Division, Smith Kline & French Laboratories, King of Prussia, Pennsylvania 19406

Received January 8, 1988; Revised Manuscript Received March 14, 1988

ABSTRACT: X-ray absorption edge and extended X-ray absorption fine structure (EXAFS) spectra are reported for the Cu(I) and Cu(II) forms of bovine dopamine β-hydroxylase (DBH; EC 1.14.17.1) and for the Cu(I) form of DBH bound either to tyramine substrate or to a multisubstrate inhibitor [Kruse, L. I., DeWolf, W. E., Jr., Chambers, P. A., & Goodhart, P. J. (1986) *Biochemistry 25*, 7271–7278]. A significant change in the structure of the copper sites occurs upon ascorbate-mediated reduction of Cu(II) DBH to the Cu(I) form. While the average Cu(II) site most likely consists of a square-planar array of four (N,O)-containing ligands at 1.98 Å, the average Cu(I) site shows a reduction in (N,O) coordination number (from ~4 to ~2) and the addition of a S-containing ligand at 2.30 Å. No change in the average Cu(I) ligand environment accompanies binding of tyramine substrate, whereas binding of a multisubstrate inhibitor, 1-(3,5-difluoro-4-hydroxybenzyl)-1*H*-imidazole-2(3*H*)-thione, causes an increase in the Cu–S coordination, consistent with inhibitor binding to the Cu(I) site through the S atom. Although excellent signal-to-noise ratio in the EXAFS spectra of ascorbate-reduced DBH facilitated analysis of outer-shell scattering for a Cu···Cu interaction, the presence of a binuclear site could not be proven or disproven due to interference from Cu···C scattering involving the carbons of imidazole ligands.

Dopamine β-hydroxylase (DBH;[1] EC 1.14.17.1) is a copper-containing monooxygenase that catalyzes the benzylic hydroxylation of dopamine to norepinephrine (Skotland & Ljones, 1979; Rosenberg & Lovenberg, 1980; Villafranca, 1981; Ljones & Skotland, 1984). In spite of the physiological importance of this biotransformation (Kruse et al., 1986a) and the interesting dependence of the monooxygenase activity upon prosthetic copper ions, surprisingly little is known about the ligand environment of the active site copper atoms in DBH (Kruse et al., 1986b). Indeed, even the copper:protein stoichiometry has been an issue for debate although recent studies have convincingly demonstrated that a 2:1 copper:subunit stoichiometry leads to maximal catalysis for phenethylamine substrate (Klinman et al., 1984) or alternative substrates (Ash et al., 1984). Catalysis by DBH follows a priming of the enzyme by reduction of the Cu(II) form to the Cu(I) form by a one-electron donor (Rosenberg & Lovenberg, 1980;

† Supported by National Science Foundation Grant DMB 85-02707 (to R.A.S.). The XAS work reported herein was performed at the Stanford Synchrotron Radiation Laboratory, which is supported by the Office of Basic Energy Sciences, Department of Energy, and the Biotechnology Resource Program, Division of Research Resources, National Institutes of Health. R.A.S. is a Presidential Young Investigator and an Alfred P. Sloan Research Fellow.

* Authors to whom correspondence should be addressed.
‡ University of Georgia.
§ University of Illinois.
∥ Smith Kline & French Laboratories.
⊥ Present address: Department of Medicinal Chemistry, Smith Kline & French Research Limited, The Frythe, Welwyn, Hertfordshire, England AL6 9AR.

[1] Abbreviations: DBH, dopamine β-hydroxylase; EPR, electron paramagnetic resonance; EXAFS, extended X-ray absorption fine structure; FT, Fourier transform; HPLC, high-performance liquid chromatography; XAS, X-ray absorption spectroscopy.

0006-2960/88/0427-5411$01.50/0